Acta Metallurgica Sinica (English Letters) (2023) 36:495–506
https://doi.org/10.1007/s40195-022-01491-7

Impacts of Microalloying Elements on the Hardening β"-Phase in Automotive AlMgSi Alloys

Zhaoqun Chen[1] · Yuxiang Lai[1] · Linghong Liu[2] · Ziran Liu[3] · Jianghua Chen[1]

Received: 24 April 2022 / Revised: 28 July 2022 / Accepted: 5 September 2022 / Published online: 3 December 2022

Abstract
Microalloying elements play a crucial role in mechanical properties and phase stability of metallic alloys. In this work, we employ first-principles calculations and atomic-scale high-angle annular dark-field scanning transmission electron microscopy (HAADF-STEM) to find promising microalloying elements that will improve the stability and properties of β"/Al interface and β" phase in Al–Mg-Si alloys. First, we define a substitution energy for evaluating the stability of β" phase and β"/Al interface with microalloying elements doped. Then, experiments of HAADF-STEM imaging are carried out to verify the calculational results. Next, using the most stable structures doped with microalloying elements, the mechanical properties of the β" bulk and the β"/Al interface were calculated and analyzed. At last, we have figured out the effects of all considered microalloying elements and obtained a rule that the stable occupancy of solute atoms is related to their own radius and the radius of Mg, Si, and Al. These findings will provide some theoretical basis for future microalloying strategies of Al–Mg-Si alloys.

Keywords Al–Mg-Si alloy · Microalloying · Precipitate · Crystal structure · Elastic properties · First-principles calculations

1 Introduction

Al–Mg-Si alloys have been widely applied in aerospace, aviation, and automobiles due to their high strength-to-weight ratio, excellent corrosion resistance and formability, and low cost [1–3]. The strengthening of Al–Mg-Si alloys is achieved mainly by a large number of dispersed nano-sized precipitates formed during aging process, which can effectively impede the dislocation movement. The crystal structure, size, number density, and volume fraction of the precipitates have significant effects on the mechanical properties of the alloys. The well-accepted precipitation sequence of Al–Mg-Si alloys is described as [4–6]: supersaturated solid solution (SSSS) → clusters → GP zones/pre-β" → β" → β' (/B'/U1/U2) → β.

The β" phase, mostly formed at the peak-aging condition, is the most effective hardening phase in Al–Mg-Si alloys. The monoclinic β" has lattice parameters of $a = 1.516$ nm, $b = 0.405$ nm, $c = 0.674$ nm, $\beta = 105.3°$ [7]. The orientation relationships between β" and the Al-matrix are $[230]_{Al}$ // $[100]_{\beta"}$, $[001]_{Al}$ // $[010]_{\beta"}$, and $[3\ 10]_{Al}$ // $[001]_{\beta"}$ [7, 8]. The composition of β" was first determined as Mg_5Si_6 by dynamic electron diffraction [9]. Recent atom probe tomography and energy-dispersive X-ray spectroscopy studies suggested that the β" phase contains some Al [10–13]. First-principles calculations indicated that $Mg_5Al_2Si_4$ is the most likely β" composition among the $Mg_{5-x}Si_{6-y}Al_{x+y}$ ($0 \le x \le 5$, $0 \le y \le 6$) compositions [12]. Hence, the composition of β" is still a subject of controversy.

Adding microalloying elements is an efficient method to enhance the mechanical properties of Al–Mg-Si alloys. Available experimental studies have shown that the improvement of properties by the addition of

Available online at http://link.springer.com/journal/40195.

✉ Yuxiang Lai
lyxzhc123@hnu.edu.cn

✉ Ziran Liu
zrliu@hunnu.edu.cn

[1] Center for High-Resolution Electron Microscopy, College of Materials Science & Engineering, Hunan University, Changsha 410082, Hunan, China

[2] College of Science, Central South University of Forestry and Technology, Changsha 410004, China

[3] Department of Physics and Key Laboratory for Low-Dimensional Structures and Quantum Manipulation (Ministry of Education), Hunan Normal University, Changsha 410081, China

microalloying elements is mostly related to microstructure changes of the β'' phase [14–24]. High-angle annular dark-field scanning transmission electron microscopy (HAADF-STEM) studies on the effect of Cu addition on the precipitation of Al–Mg-Si alloys have shown that Cu can enter the β'' phase and replace the Al atoms [14]. The effect of Zn on the structure of the β'' phase is similar to that of Cu, i.e., Zn atoms also occupy the Al sites of the β'' phase [15–17]. Atomic-scale HAADF-STEM characterization of the precipitates of Al–Mg-Si-Ge alloys revealed that Ge atoms can occupy the Si1 and Si2 sites, usually the Si2 site of the β'' phase [18, 19]. Moreover, Cu, Zn, and Ge atoms can also segregate at the β''/Al interface [16, 17, 19, 20]. It was also found that the addition of Cu, Zn, and Ge to Al–Mg-Si alloy can effectively refine the size of the β'' phase and increase its number density through entering the β'' phase, thereby increasing the strength of the alloy [16, 18, 21]. Compared with Cu, Zn, and Ge, Ag can segregate at the β''/Al interface but does not enter the β'' phase [22, 23]. Recently, we have reported that the addition of Sc makes disordered β'' precipitate in the peak-aged Al–Mg-Si alloys, and Sc atoms are located at the precipitate/matrix interface and in the disordered regions, but they do not occupy the atomic sites of the β'' phase [24]. Although the effect of microalloying element addition on the β'' structure and the properties of Al–Mg-Si alloys has received much attention, the types of microalloying elements involved in previous studies have been limited. Moreover, there have been no systematic comparisons of the impacts of different microalloying elements on the structure or properties of the β'' phase. It has been demonstrated that first-principles calculations provide an efficient approach for establishing precipitate energetics and for evaluating their mechanical properties [25–29].

In the present work, using first-principles calculations and atomic-resolution HAADF-STEM, influences of a variety of microalloying elements on the stability and properties of β''/Al interface and β'' phase were investigated. We define a substitution energy for calculating the energy difference of β'' phase and β''/Al interface with microalloying elements doped. Then, experiments of HAADF-STEM imaging are carried out to verify the calculational results. Using the most stable structures doped with microalloying elements, the mechanical properties of the β'' bulk and the β''/Al interface were evaluated and analyzed. Our results provide scientific data for developing new Al–Mg–Si alloys with microalloying elements, as well as to further understanding the relationship between material structure and its performance.

2 Methodology

2.1 Calculation Details

The β'' unit cell model and two types of β''/Al interface models were built for the first-principles calculations, as shown in Fig. 1. The interface normal to $[001]_{Al}$ was not considered in this work due to the high interfacial energy [30]. For the considered interface structures, a sandwich supercell of Al/β''/Al consisting of two 7-layer Al slabs and a β'' slab was

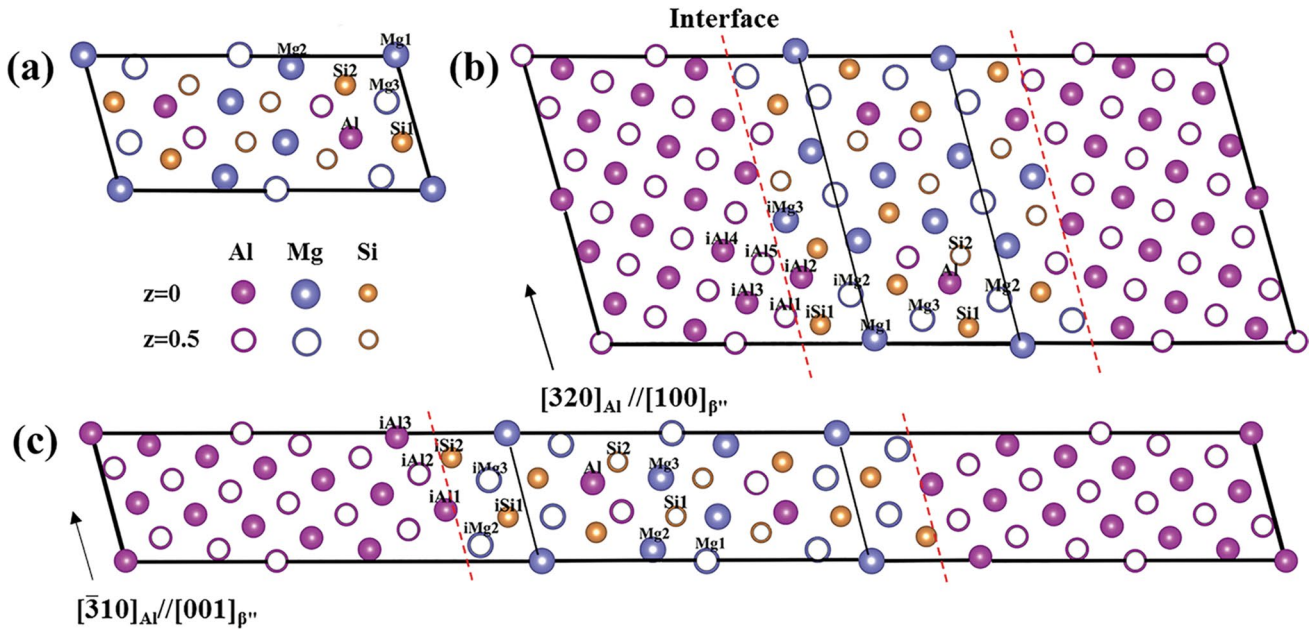

Fig. 1 Structure models for the first-principles calculations of this work: **a** β'' unit cell model, **b** β''/Al interface model along $[230]_{Al}$, **c** β''/Al interface model along $[3\ 10]_{Al}$

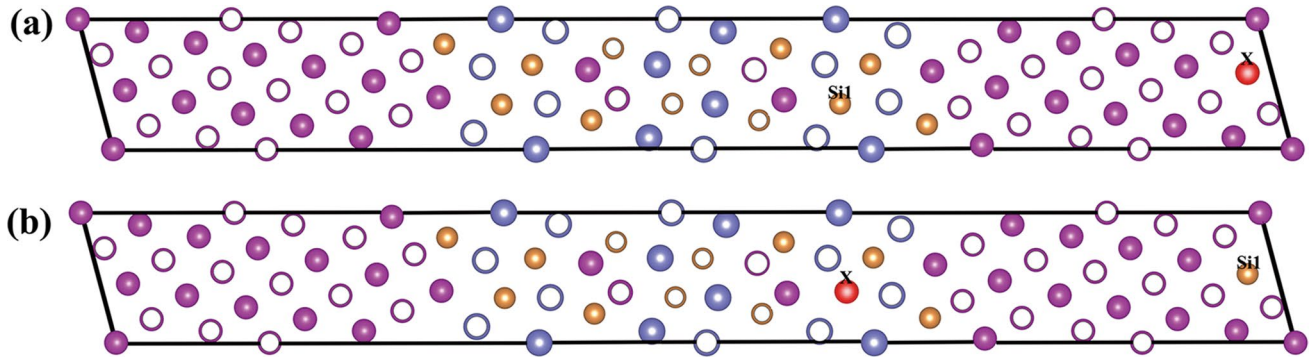

Fig. 2 Supercells used for calculating the substitution energy of one solute atom X at the Si1 site in the β"/Al interface along $[\bar{3}\ 10]_{Al}$: **a** Supercell for calculating $E^1_{Al_{52}Mg_{15}Si_{12}X}$ with X located at matrix Al, **b** the same supercell of **a** with X and Si1 exchanged

used after convergence tests. The 34 microalloying elements studied in this paper are divided into three categories according to their properties: (1) elements that strongly bound to vacancies (Type I) [31], including Ag, Cd, Pt, Na, Ca, In, Pb, Ge, Sb, Sn, and Zn; (2) elements that bind strongly to Mg or Si (Type II) [31], including Zr, Ti, V, Mn, Fe, Co, Nb, and Cu; (3) rare earth elements (Type III), including Sc, La, Ce, Pr, Nd, Pm, Sm, Eu, Gd, Tb, Dy, Ho, Er, Tm, and Yb. Note that the three types of elements may overlap each other. For example, the third type of the rare earth element Sc can bind strongly to Si, while this property belongs to the second type of elements.

To investigate the effect of microalloying elements on the stability of β" bulk and β"/Al interface, the substitution energy of each microalloying element was calculated by replacing different atomic sites in two types of β"/Al interface models (Fig. 1b and c) with microalloying elements. The atomic sites in the β"/Al interface structure models are divided into two categories: β" interfacial sites and β" bulk sites. The sites in the two nearest layers of the β"/Al interface were named as iAl1, iAl2, etc., while other sites, Mg1, Mg2, Mg3, Si1, Si2, and Al, were referred to the β" bulk sites.

All the first-principles calculations in this paper were carried out on the Vienna Ab initio Simulation Package (VASP) code [32, 33]. The valence electrons were described using the generalized gradient approximation (GGA) with the exchange–correlation function of Perdew, Burke, and Ernzerhof (PBE) [34]. The interaction between ions and core electrons was described by the projector augmented wave (PAW) method [32]. Convergence tests indicated that a cutoff energy of 400 eV was sufficient to ensure convergence of energy within 1×10^{-5} eV/atom. The Brillouin-zone gridding was performed using the Monkhorst–Pack method [35], and the k-point meshes are $3\times9\times7$ for the β"/Al interface structure models and $3\times11\times7$ for the β" unit cell model.

The substitution energy (E_{sub}) of the microalloying element X is defined as the energy required for a solute X dissolved in the Al-matrix replacing a site at the β"/Al interface or in the β" bulk [36, 37]. As an example, the E_{sub} of element X at the Si1 site in the β"/Al interface along $[3\ 10]_{Al}$ was defined as:

$$E_{sub}=E^2_{Al_{52}Mg_{15}Si_{12}X}-E^1_{Al_{52}Mg_{15}Si_{12}X}, \quad (1)$$

where $E^1_{Al_{52}Mg_{15}Si_{12}X}$ is the total energy of the supercell with one solute atom X dissolving in the Al-matrix (Fig. 2a). $E^2_{Al_{52}Mg_{15}Si_{12}X}$ is the total energy of the same supercell as Fig. 2a with X and Si1 exchanged, as shown in Fig. 2b. A negative substitution energy means relative stable structure with the addition of element X, i.e., an energetically favorable substitution with X.

To study the effect of microalloying elements on the adhesion of the β"/Al interface, the β"/Al interface models with and without microalloying elements occupying their favorable atomic sites were built to calculate the adhesion energy. The work of adhesion (W_{ad}) for the β"/Al interface is defined as the reversible work needed to separate the interface into two free surfaces [38, 39]:

$$W_{ad}=\left(E_{Al}+E_{\beta''}-E_{\beta''/Al}\right)/A, \quad (2)$$

where E_{Al} and β" are the total energies of the relaxed, isolated Al and β" slabs in the same supercell when one of the slabs is retained and the other is replaced by a vacuum, respectively. β"/Al is the total energy of the β"/Al interfacial supercell. A is the area of the interface β"/Al.

The elastic properties can be derived from the elastic stiffness constants C_{ij} and the elastic compliance constants S_{ij} [40–42], where $[S_{ij}]$ is the inverse matrix of $[C_{ij}]$ [43]. There are nine independent elastic stiffness constants (C_{11}, C_{22}, C_{33}, C_{44}, C_{55}, C_{66}, C_{12}, C_{13}, and C_{23}) in the β" monoclinic structure. Hill [42] proposed that the modulus obtained from

the Voigt and Reuss approximations is usually the upper and lower limits of the actual effective modulus, respectively. Within the Voigt–Reuss–Hill approximation, the expressions of the bulk modulus (B), shear modulus (G), Young's modulus (E), and Poisson's ratio (ν) are as follows:

$$B_V = \left[\left(C_{11} + C_{22} + C_{33}\right) + 2\left(C_{12} + C_{13} + C_{23}\right)\right]/9, \quad (3)$$

$$G_V = \left[\left(C_{11} + C_{22} + C_{33}\right) - \left(C_{12} + C_{13} + C_{23}\right) + 3\left(C_{44} + C_{55} + C_{66}\right)\right]/15, \quad (4)$$

$$B_R = \left[\left(S_{11} + S_{22} + S_{33}\right) + 2\left(S_{12} + S_{13} + S_{23}\right)\right]^{-1}, \quad (5)$$

$$G_R = 15/\left[4\left(S_{11} + S_{22} + S_{33}\right) - 4\left(S_{12} + S_{13} + S_{23}\right) + 3\left(S_{44} + S_{55} + S_{66}\right)\right], \quad (6)$$

$$B_H = \frac{1}{2}\left(B_V + B_R\right), \quad (7)$$

$$G_H = \frac{1}{2}\left(G_V + G_R\right), \quad (8)$$

$$E = \frac{9B_H G_H}{3B_H + G_H}, \quad (9)$$

$$\nu = \frac{3B_H - 2G_H}{2(3B_H + G_H)}, \quad (10)$$

where B_V and B_R are the bulk modulus calculated using the Voigt and Reuss approximations, respectively. G_V and G_R are the shear modulus calculated using the Voigt and Reuss approximations, respectively. B reflects a material's ability to resist compression deformation, G reflects its ability to resist shear strain, and E reflects its ability to resist the normal strain. Generally, the greater the G and E of a material, the greater the stiffness of the material. The ratio of B to G (B/G) and ν can be used as a criterion for determining the brittleness and ductility of materials. According to the

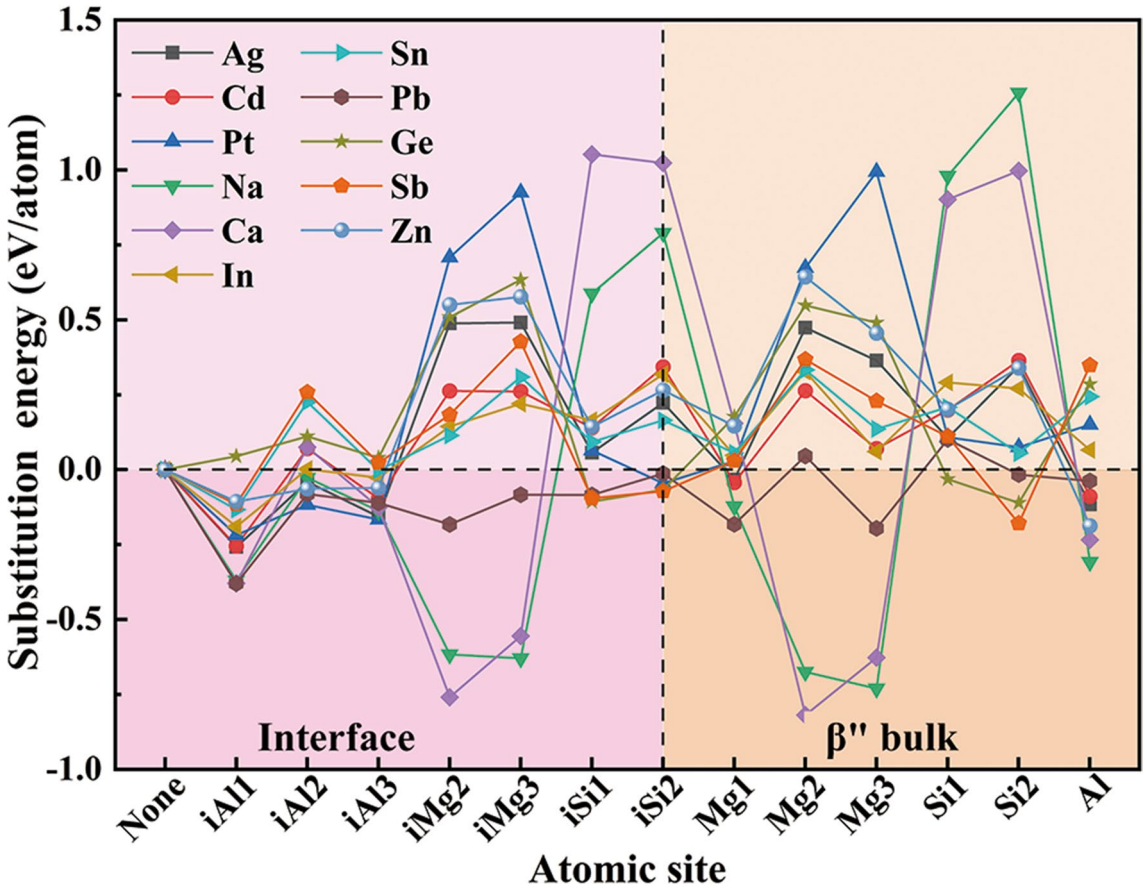

Fig. 3 Substitution energies of Type I microalloying elements at the β"/Al interface along $[\bar{3}\,10]_{Al}$

Pugh criterion [44], when $B/G > 1.75$, a material behaves in a ductile manner; otherwise, the material is brittle. ν is known as the transverse deformation coefficient. The larger the transverse deformation coefficient of a material, the better the ductility of the material [45].

2.2 Experimental

To check the occupation of Zn and Sc in the β" bulk and at the β"/Al interface, the precipitate microstructures of two alloys with chemical compositions of Al-0.48 Mg-0.99Si-2.98Zn (wt%) and Al-1.4 Mg-0.5Si-0.2Sc (wt%) were characterized. The ingots were homogenized at 500 °C for 10 h, hot- and cold-rolled to 1-mm-thick sheets, solution treated at 565 °C for 30 min, water quenched to room temperature, and immediately aged in an oil bath at 180 °C. Atomic-scale HAADF-STEM characterization was performed on an aberration-corrected FEI Titan Cubed Themis G2 transmission electron microscope (TEM) at 300 kV with the electron beam parallel to the $<100>_{Al}$ directions. TEM specimens were prepared by twin-jet electro-polishing using a Struers Tenupol 5 machine with an electrolyte of 1/3 HNO_3 in methanol at a temperature of about − 30 °C.

3 Results and Discussion

3.1 Stability of β" Bulk and β"/Al Interface

3.1.1 First-Principles Calculations

Figure 3 shows the calculated substitution energies with Type I microalloying elements at the β"/Al interface along $[3\ 10]_{Al}$. First, for the interfacial sites, Ag, Cd, Pt, In, Sn, Pb, Sb, and Zn have negative and lowest substitution energies at the Al1 site, indicating that the Al1 site is the most preferential site of these elements. Nevertheless, Na, Ca, and Ge exhibit the strongest preference for the interfacial Mg3, Mg2, and Si1 sites, respectively. Then, for the β" bulk sites, the most preferential sites for Ag, Cd, Pb, Sb, Zn, Na, Ca, and Ge are the Al, Al, Mg3, Si2, Al, Mg3, Mg2, and Si2 sites, respectively. However, the substitution energies of Pt, In, and Sn at all the β" bulk sites are positive, implying that these three elements have no preference for entering the β" bulk. Finally, comparing the substitution energies of each microalloying element at the interface with those in the β" bulk, Ag, Cd, Pt, In, Sn, and Pb have the lowest substitution energies at the interfacial Al1 site, indicating that the

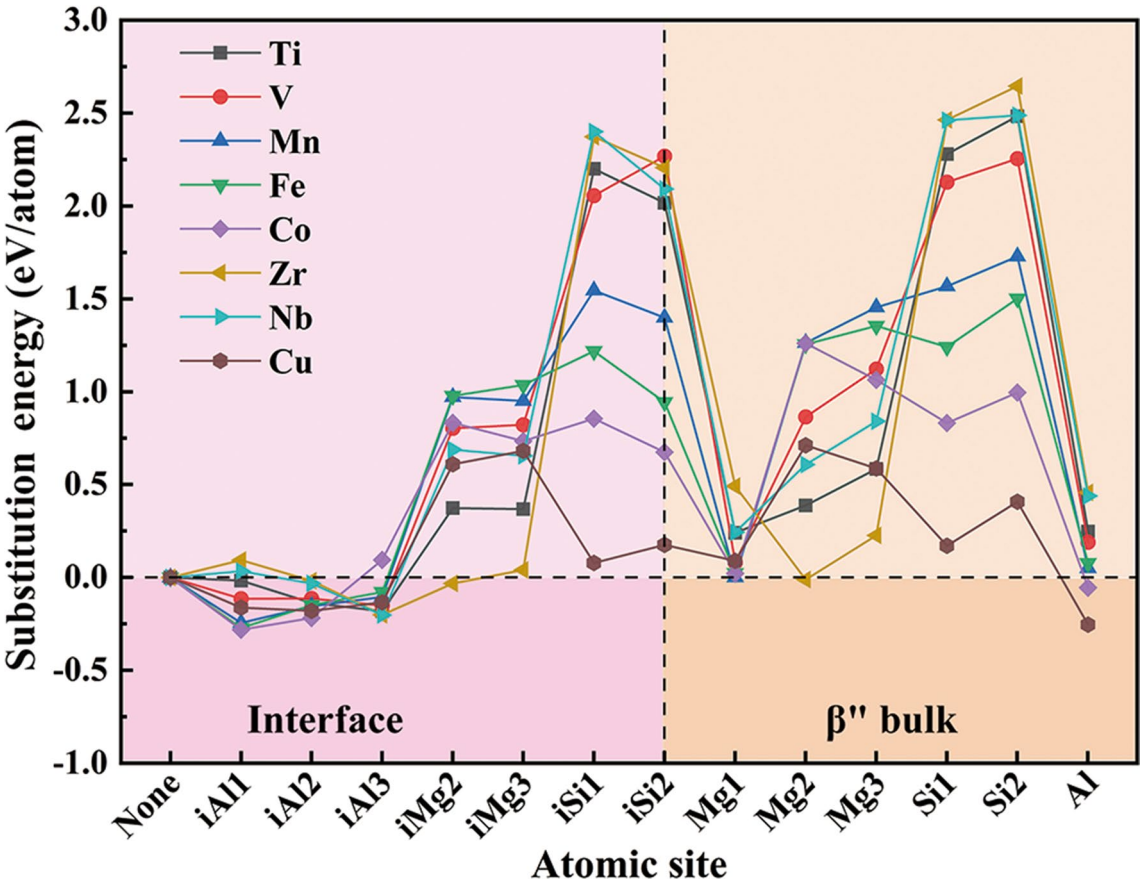

Fig. 4 Substitution energies of Type II microalloying elements at the β"/Al interface along $[\bar{3}\ 10]_{Al}$

interfacial Al1 site is preferred for these elements over their preferential β" bulk sites. In contrast, Sb, Zn, Na, Ca, and Ge have the lowest substitution energies at the sites of β" bulk, which means that these elements are more inclined to enter the β" phase. According to the classical nucleation theory, the growth of precipitates is governed by the diffusion of solute atoms from the precipitate/matrix interfaces into the precipitates. Additionally, the substitution energies of Sb, Zn, Na, Ca, and Ge at the most preferential interfacial sites are only somewhat higher than the corresponding substitution energies at the most preferential β" bulk sites. Therefore, the segregations of Sb, Zn, Na, Ca, and Ge at the β"/Al interface are presumed.

Figure 4 shows the substitution energies of Type II microalloying elements at the β"/Al interface along $[3\ 10]_{Al}$. Among the interfacial sites, the Al sites are the most preferential sites for all of the Type II microalloying elements. For the β" bulk sites, the Mg2, Al, and Al sites are the most preferred for Zr, Co, and Cu, respectively, but Ti, V, Mn, Fe, and Nb have no preference for entering the β" bulk due to their positive substitution energies at all the β" bulk sites. Zr, Ti, V, Mn, Fe, Co, and Nb prefer to the interfacial Al sites rather than β" bulk sites. Nevertheless, Cu prefers to the Al site in the β" bulk and Al2 site in the β"/Al interface.

The substitution energies of rare earth (Type III) microalloying elements at the β"/Al interface along $[3\ 10]_{Al}$ are shown in Fig. 5. Among the interfacial sites, the Mg2 site is the most preferential site for all of the rare earth elements, while among the β" bulk sites, the Mg2 site is the most preferred substitution site for all the rare earth elements. When the substitution energies at the interface are compared to those in the β" bulk, Sc, La, Ce, Pr, Nd, Pm, Sm, Eu, Gd, Tb, Dy, and Ho prefer the interfacial Mg2 site rather than the Mg2 site in the β" bulk. On the contrary, Er, Tm, and Yb prefer the Mg2 site in the β" bulk than the interfacial Mg2 site. These three elements are also expected to segregate to the interfacial Mg2 site.

The effects of microalloying elements on the stability of β" bulk and β"/Al interface are consistent for both interface structure models, except for Na. The substitution energies of three types of microalloying elements at the interfacial sites of the structure model of β"/Al interface along $[230]_{Al}$ are displayed in Fig. 6. Na prefers to occupy the Mg3 site in the β" bulk and to the β"/Al interfaces in both interface models,

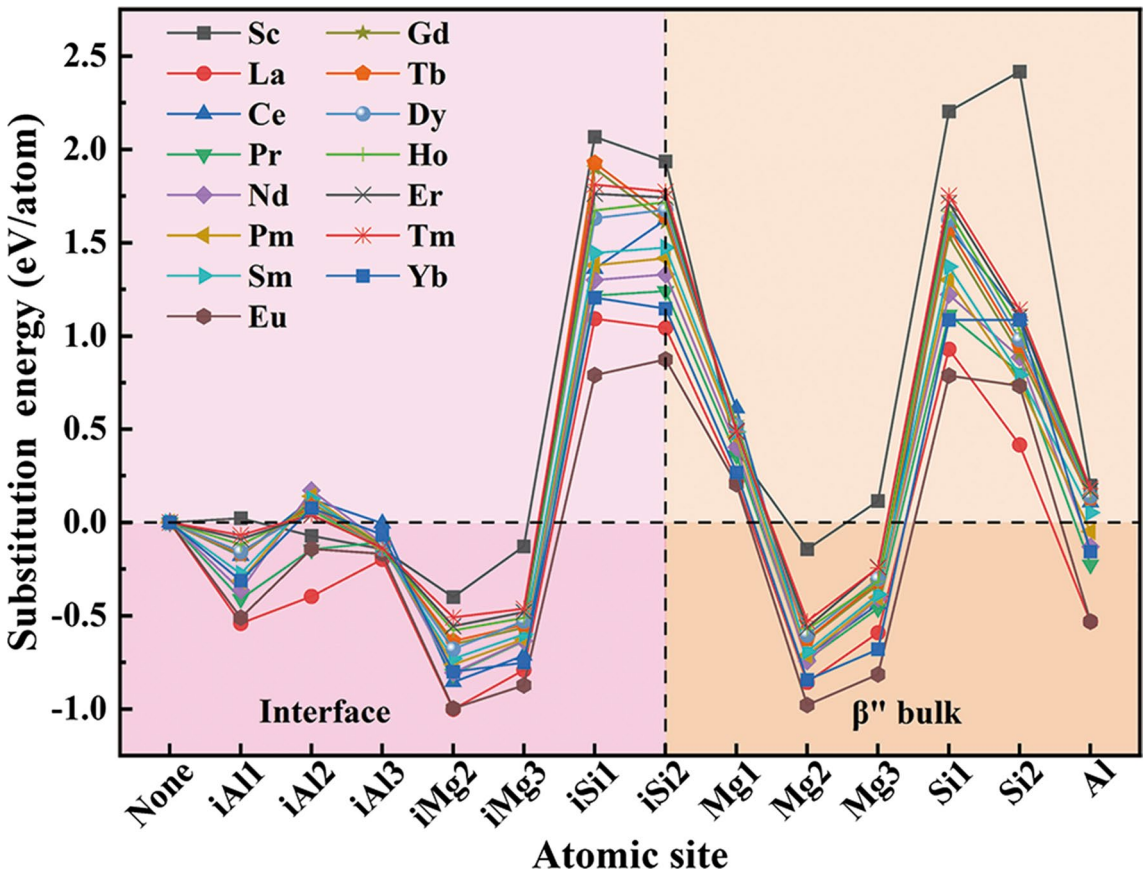

Fig. 5 Substitution energies of Type III microalloying elements at the β"/Al interface along $[\bar{3}\ 10]_{Al}$

but the most preferred segregation site differs for the two interfaces (the interfacial Mg3 site for the interface along $[3\ 10]_{Al}$ and the interfacial Mg2 site for the interface along $[230]_{Al}$). This difference could be caused by the calculation errors. As shown in Figs. 3 and 6a, the substitution energy of Na at the interfacial Mg2 site and that at the interfacial Mg3 site are quite close in both interface models. The substitution energies of microalloying elements in the β" bulk exhibit similar trends as those of the β" bulk sites in the interface models (Fig. 7). The most preferential β" bulk site for each microalloying element is the same for the three structure models.

According to our calculation results (Figs. 3–7), certain rules exist between the type of atom substituted by the microalloying element X and the atomic radius of X (R_X). By their atomic radius [46], the microalloying elements studied in this study are divided into three categories: (1) elements with $R_X > R_{Mg}$ (1.60 Å), including Sc, La, Ce, Pr, Nd, Pm, Sm, Eu, Gd, Tb, Dy, Ho, Er, Tm, Yb, Na, and Ca. Such elements tend to occupy the Mg sites. (2) Elements with R_{Al} (1.43 Å) $< R_X \leq R_{Mg}$, including Ag, Cd, In, Sn, Zr, Ti, and Nb. Such elements tend to occupy the Al or Mg sites. (3) Elements with R_{Si} (1.18 Å) $< R_X \leq R_{Al}$, including Zn, Cu, Pt, Ge, V, Mn, Fe, and Co tend to occupy the Si or Al sites. However, in the case of Sb, the above criteria are not met. Sb has a slightly larger radius than Mg, but it prefers the Si site, indicating that, besides atomic radius, there are other factors that determine the influence of microalloying elements on precipitate structures, which will be explained in Sect. 3.2.2.

3.1.2 Experimental Verification

The substitution energy calculation results have shown that all the microalloying elements studied exhibit a preference for segregating at specific positions at the β"/Al interface. Previous experimental studies have reported the segregation of Ge, Zn, Cu, Ag, and Sc at the β"/Al interface [16, 19, 20, 22, 24], which is consistent with the calculations of the present work. Our calculations have also shown that only some of the microalloying elements have strong tendency to enter the β" bulk. Experimental studies have demonstrated that Ge, Zn, and Cu occupy the Si2, Al, and Al sites of the β"

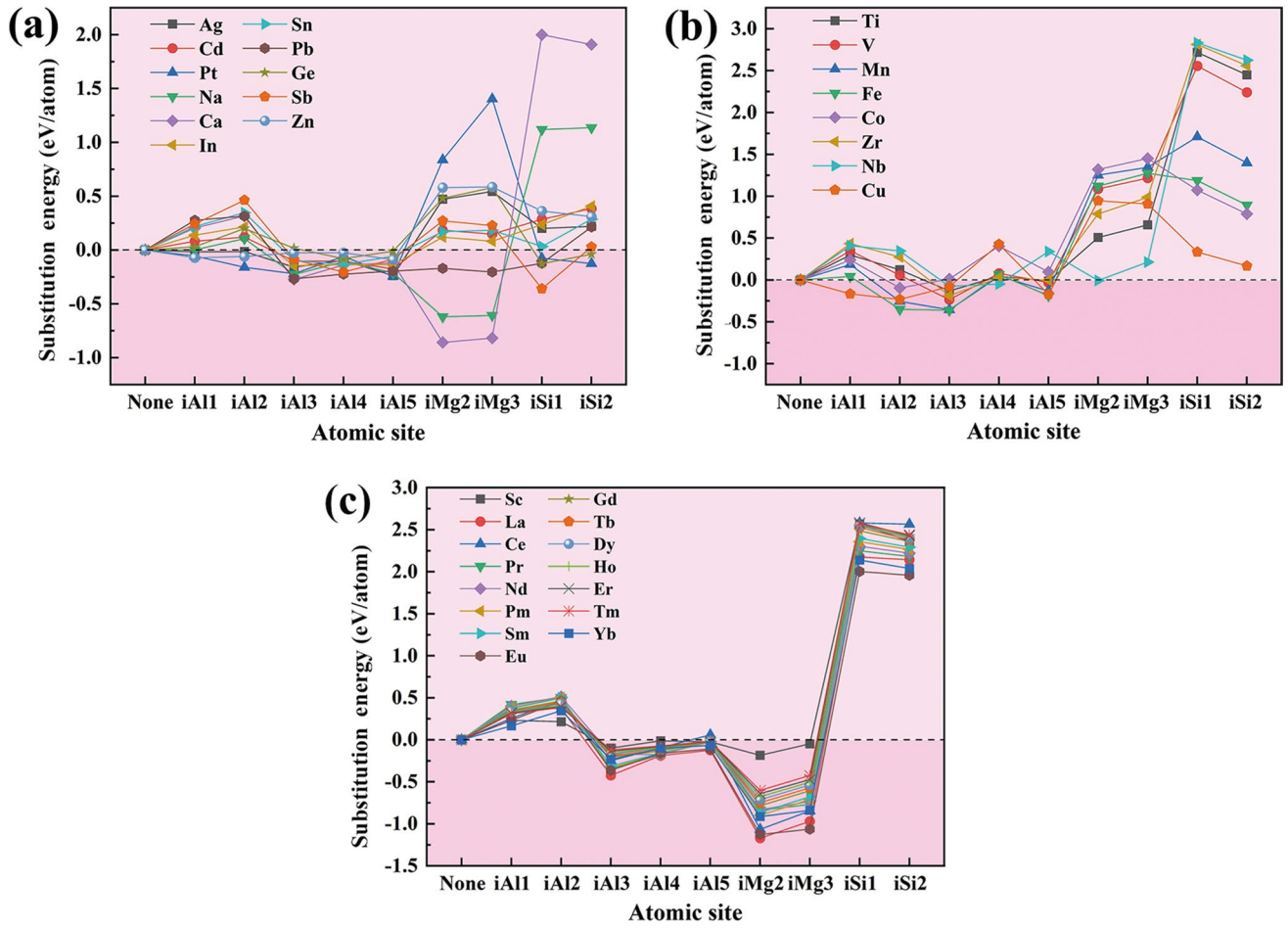

Fig. 6 Substitution energies of three types of microalloying elements at the β"/Al interface along $[230]_{Al}$: **a** Type I elements, **b** Type II elements, **c** Type III elements

phase, respectively [15, 19, 20], which is in good agreement with the calculations of the present study. In the case of Zn, for example, the atomic-resolution HAADF-STEM image of the β'' precipitate formed in the Zn-added Al–Mg-Si alloy, as presented in Fig. 8a, clearly shows that Zn atoms occupy the Al site of the β'' structure (indicated by the orange dashed ellipses) and segregate at the interfacial Al sites of the β''/Al interfaces along $[230]_{Al}$ and $[3\ 10]_{Al}$ (indicated by the blue arrows) [17]. Er, Tm, Yb, Na, Ca, and Sb, in addition to the three elements that have been experimentally verified [15, 19, 20], are also predicted to enter the β'' bulk, with Er, Tm, Yb, and Ca most preferring the Mg2 site, Na the Mg3 site, and Sb the Si2 site of the β'' structure. Elements with a significant tendency to substitute certain atomic sites in the β'' bulk are expected to facilitate the formation of the β'' precipitate and hence have a beneficial effect on the age hardening potential of Al–Mg-Si alloys.

Our previous work [24] demonstrated that, despite the fact that Sc atoms cannot enter the β'' structure, Sc-containing disordered regions connecting to the β'' structure frequently occur in the β'' precipitates formed in Sc-added Al–Mg-Si alloys due to the strong binding between Sc and Si atoms [31]. Upon further aging, the disordered β'' precipitates gradually evolve into the β''-related composite precipitates (Fig. 8b), rather than the β' precipitates, thus improving the thermal stability of the alloys. Considering this phenomenon, adding elements that cannot enter the β'' bulk and strongly bind to Si or Mg, such as Sc and Zr, to Al–Mg-Si alloys is predicted to enhance the thermal stability of the alloys.

3.2 Mechanical Properties of β'' Phase and β''/Al Interface

3.2.1 Adhesion of β''/Al Interface

Figure 9 shows the calculated W_{ad} values for the β''/Al interface along $[3\ 10]_{Al}$ with microalloying elements occupying their most preferential atomic sites. The W_{ad} for this interface without microalloying elements with a value of 2.516 J/m^2 is also given for comparison. The W_{ad} increases when Pt, Zr, Ti, V, Mn, Fe, Co, Nb, and Cu occupy the interfacial

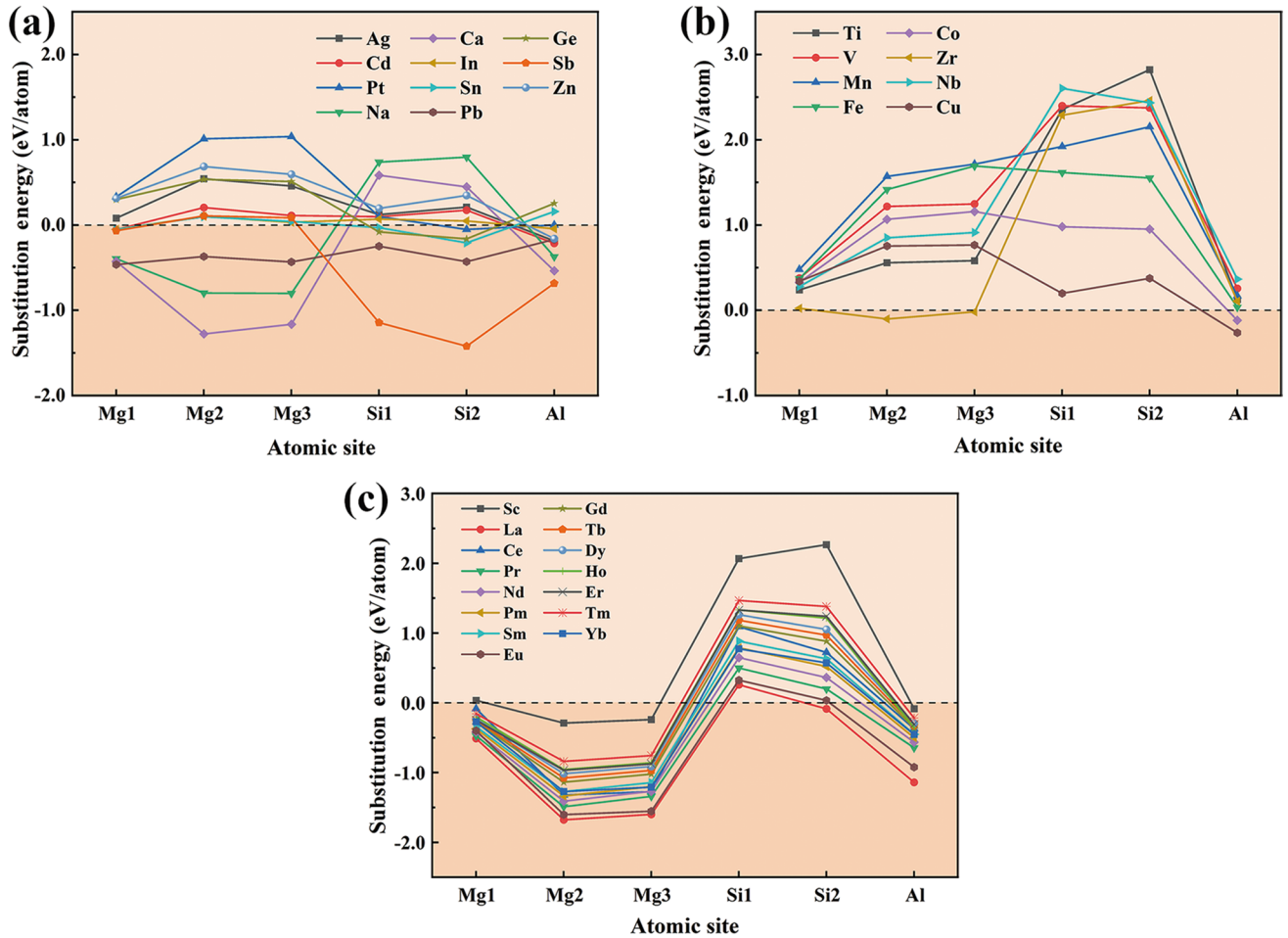

Fig. 7 Substitution energies of three types of microalloying elements in the β'' bulk: **a** Type I elements, **b** Type II elements, **c** Type III elements

Al sites, as shown in Fig. 9a, indicating that the segregation of these elements to the β"/Al interface can increase the adhesion of the interface. The segregation of Ag and Zn to the interfacial Al sites shows a negligible effect on the interface's adhesion, but the segregation of Cd, In, Sn, Pb, and Sb to the interfacial Al sites reduces the interface's adhesion. For the microalloying elements with a strong preference for the interfacial Si or Mg sites, only the Ge segregation at the β"/Al interface can enhance the adhesion of the interface (see Fig. 9b). As shown in Fig. 9c, for the microalloying elements with a strong tendency to enter the β" bulk, the occupation of Ge and Sb in the β" bulk increases the adhesion of the β"/Al interface, whereas the occupation of Na, Ca, Er, Tm, and Yb in the β" bulk decreases it. The occupation of Zn and Cu in the β" bulk has little impact on the interfacial adhesion.

Given that the microalloying elements occupy their most preferred β" bulk sites and β"/Al interfacial sites, it is interesting to find that (1) solute substitution at the Si sites (in the cases of Ge and Sb) increases the adhesion of the β"/Al interface; (2) solute substitution at the Mg sites decreases the adhesion of the interface; (3) the effect of solute substitution at the Al sites on the interface's adhesion depends on the type of microalloying elements, i.e., the substitution of Pt and Type II microalloying elements at the Al sites improves the interface's adhesion, while the substitution of the other microalloying elements at the Al sites decreases or does not appreciably change the interface's adhesion.

3.2.2 Elastic Properties of β" Phase

The results of the calculation in Sect. 3.1.1 have demonstrated that Er, Tm, Yb, Ge, Na, Ca, Sb, Zn, and Cu have a strong preference for the β" bulk interior. The elastic properties of the β" phase before and after the above elements occupy their most preferential β" bulk sites were estimated using the β" unit cell model (Fig. 1a) to investigate how these elements affect the elastic properties of the β" phase. Table 1 shows the elastic stiffness constants of the β" phase without microalloying elements and those in the literature [47], which are comparable. The elastic stiffness constants of a stable crystal must satisfy the Born criterion, a mechanical stability criterion [48, 49]. This criterion specifies different restrictions on the elastic stiffness constants for different crystal structures. Except for the Sb-doped β" phase (see Table 1), the computed elastic stiffness constants show that all of the β" phases satisfy the Born criterion, indicating their mechanical stability. Although the Sb incorporation into the β" bulk is energetically favorable (Sect. 3.1.1), it makes the β" phase mechanically unstable, so it is impossible for Sb to enter β" phase forming a stable structure. Hence, the Sb-doped β" phase is ignored in the calculations of elastic properties.

The calculated elastic properties of the nine β" phase structures are shown in Fig. 10 and Table 2. According to Fig. 10a and b, the incorporation of Er, Tm, Yb, Na, Ca, Zn, and Cu results in higher G and E values of the β" phase, indicating that these elements can increase the shear strain resistance

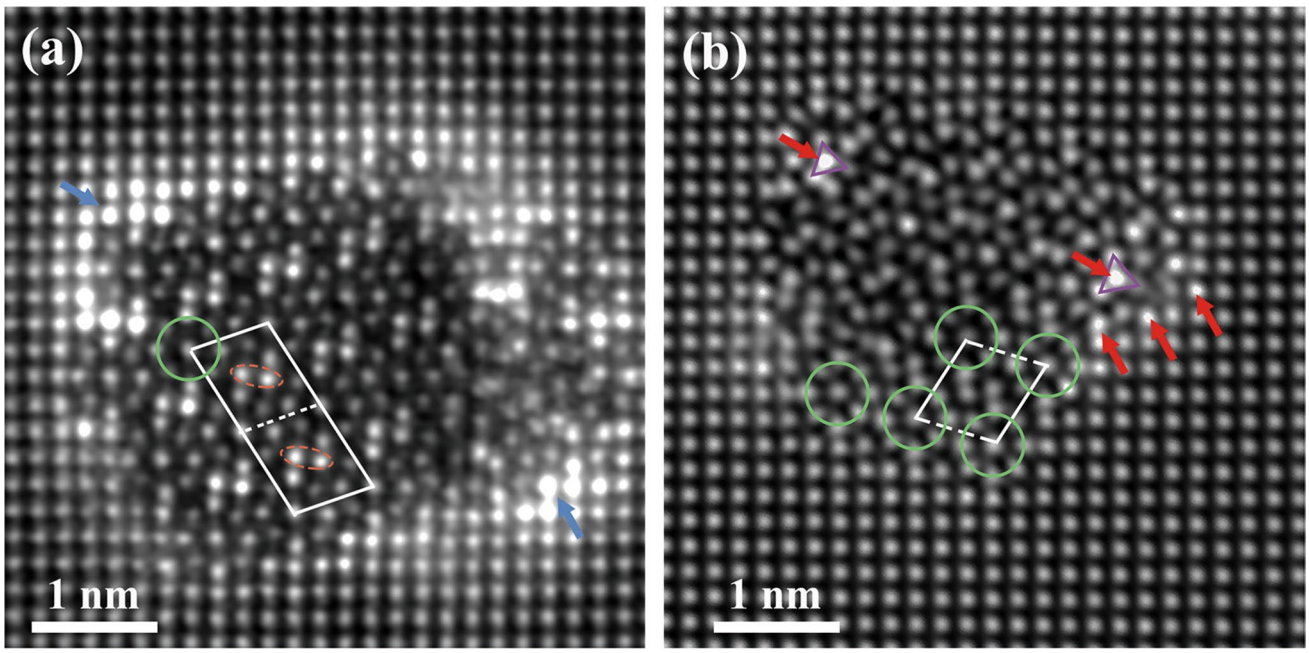

Fig. 8 Atomic-resolution HAADF-STEM images of Zn **a** and Sc **b** containing β" precipitates, taken from the Al–Mg-Si-Zn and Al–Mg-Si-Sc alloys, respectively. The green circles and purple triangles indicate the characteristic sub-units of β" and β', respectively. The blue and red arrows indicate the distinct Zn and Sc atomic columns, respectively. The orange dashed ellipses in **a** indicate the Zn-containing Al sites of the β" phase

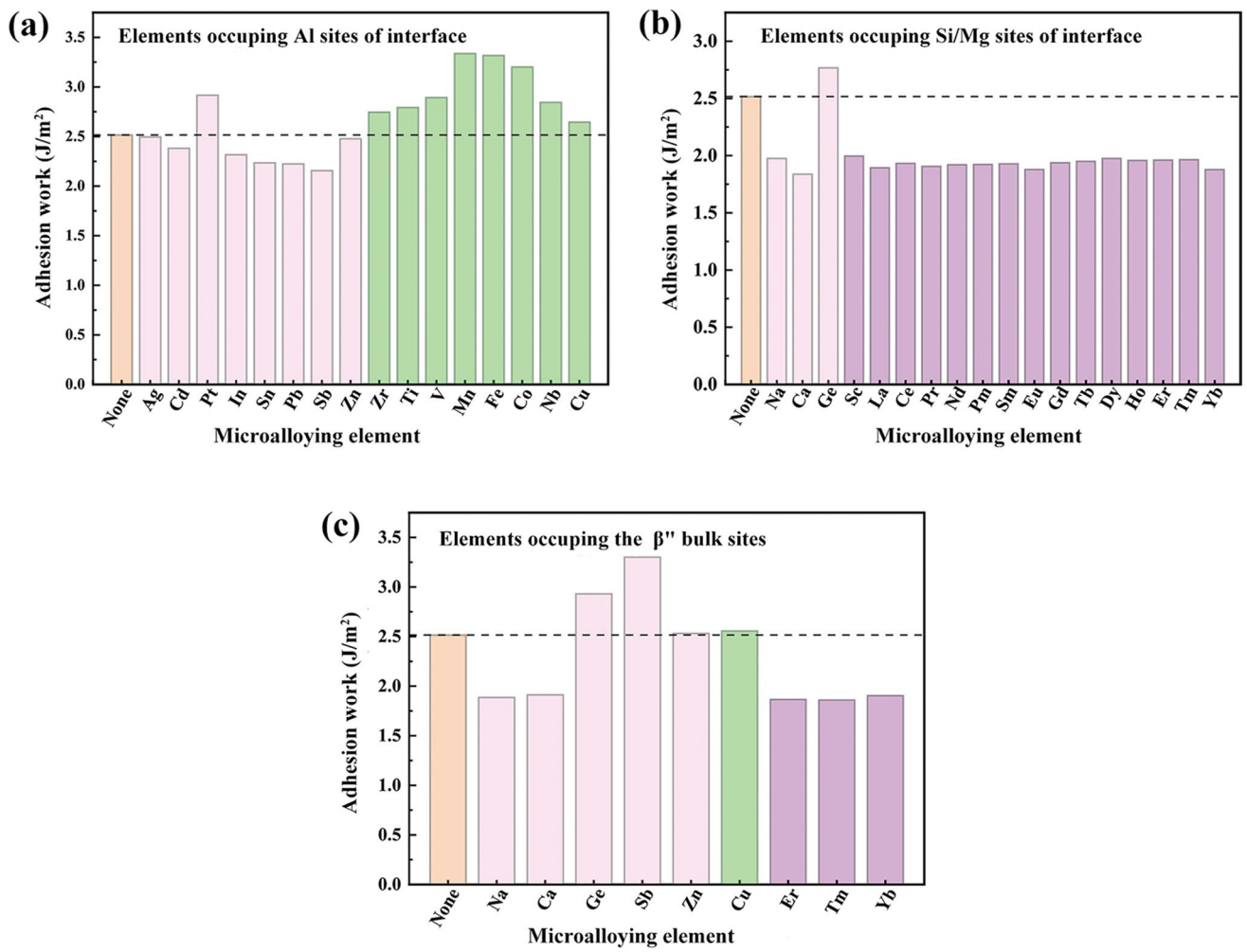

Fig. 9 Ideal work of adhesion for the β"/Al interface along $[\bar{3}\ 10]_{Al}$ with microalloying elements occupying their most preferential atomic sites: **a** the cases with microalloying elements occupying the interfacial Al sites, **b** the cases with microalloying elements occupying the interfacial Mg or Si sites, **c** the cases with microalloying elements occupying the β" bulk sites

Table 1 Elastic stiffness constants of the β" phase and Sb-doped β" phase

Phase	C_{11}	C_{22}	C_{33}	C_{44}	C_{55}	C_{66}	C_{12}	C_{13}	C_{23}
β" in Ref. [47]	108.97	89.63	98.75	26.35	27.51	32.34	49.36	43.08	57.50
β" in this work	104.74	88.08	103.21	27.59	28.14	24.49	46.33	47.31	47.00
Sb-doped β" in this work	89.22	95.79	88.31	24.63	27.03	14.29	41.56	52.06	37.82

and stiffness of the β" phase. However, the Ge incorporation reduces the shear strain resistance and stiffness of the β" phase. As shown in Fig. 10c, when Er, Tm, Zn, and Cu are incorporated into the β" bulk, the B of the β" phase increases, which means that the incorporation of these elements can enhance the compression resistance of the β" phase. In contrast, the situation is opposite for Yb, Na, Ca, and Ge. From Fig. 10d, the B/G values of all of the β" structures are larger than 1.75, indicating that they are ductile. Only the Ge incorporation increases the B/G of the β" phase, namely the ductility of the β" phase. On the contrary, the incorporation of Er, Tm, Yb, Na, Ca, Zn, and Cu reduces the ductility of the β" phase. The ν (see Fig. 10e) shows the same trend as the B/G, again demonstrating that only the incorporation of Ge enhances the ductility of the β" phase. In a brief summary, among the eight

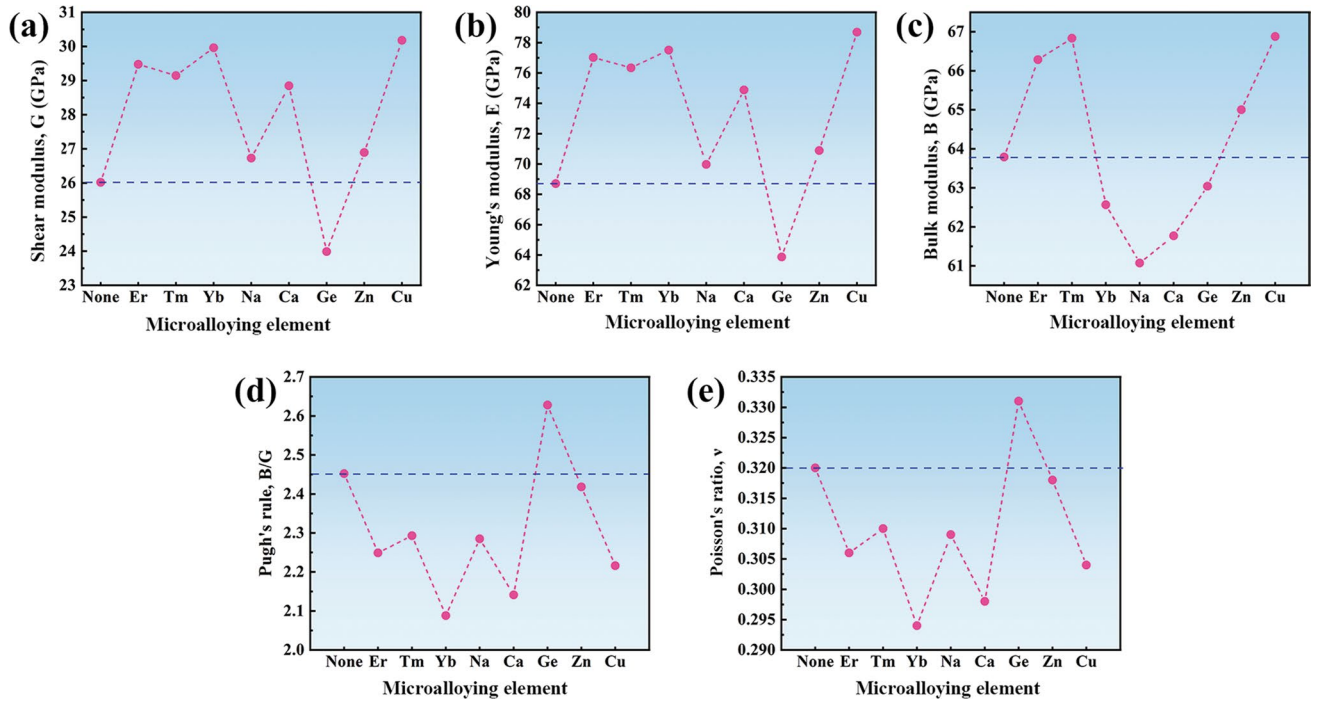

Fig. 10 Shear modulus G **a**, Young's modulus E **b**, bulk modulus B **c**, Pugh's rule B/G **d**, and Poisson's ratio ν **e** of the β" phase with microalloying elements occupying their most preferential β" bulk sites

Table 2 Elastic properties of the β" phases with and without microalloying elements occupying their most preferential atomic sites

Phase	G (GPa)	E (GPa)	B (GPa)	ν
$Mg_5Al_2Si_4$	26.02	68.71	63.79	0.320
$Mg_4Al_2Si_4Er$	29.48	77.02	66.29	0.306
$Mg_4Al_2Si_4Tm$	29.15	76.34	66.83	0.310
$Mg_4Al_2Si_4Yb$	29.96	77.51	62.57	0.294
$Mg_4Al_2Si_4Na$	26.73	69.97	61.07	0.309
$Mg_4Al_2Si_4Ca$	28.85	74.88	61.77	0.298
$Mg_5Al_2Si_3Ge$	23.99	63.87	63.04	0.331
Mg_5AlSi_4Zn	26.89	70.89	65.00	0.318
Mg_5AlSi_4Cu	30.18	78.69	66.88	0.304

microalloying elements that prefer the β" bulk, Er, Tm, Yb, Na, Ca, Zn, and Cu can improve the stiffness of the β" phase, Er, Tm, Zn, and Cu can improve the compression resistance of the β" phase, and Ge can improve the ductility of the β" phase.

4 Conclusions

Using first-principles calculations, we systematically investigated the effects of microalloying elements on the stability and properties of β"/Al interface and β" phase in Al–Mg-Si alloys and obtained the followings:

1. All microalloying elements investigated tend to segregate at the β"/Al interface, whereas Zn, Cu, Ge, Er, Tm, Yb, Na, and Ca prefer to enter the β" bulk to occupy certain atomic sites. Among them, the behaviors of Zn, Cu, and Ge have been confirmed by atomic-resolution transmission electron microscopy.
2. Segregation of Pt, Zr, Ti, V, Mn, Fe, Co, Nb, and Cu, etc., sites at the β"/Al interface and Ge occupying Si sites in the β" bulk or at the β"/Al interface can increase the interfacial bonding.
3. Regarding the influence of alloying elements on β" phase, Er, Tm, Yb, Na, Ca, Zn, and Cu can improve the stiffness of β" phase, while Ge can improve the ductility of β" phase instead.

Acknowledgements This work is financially supported by the National Natural Science Foundation of China (Nos. 52001119, 51831004, and 52171006) and the Fundamental Research Funds for the Central Universities.

Declarations

Conflict of interest The authors state that there are no conflicts of interest to disclose.

References

[1] S. Pogatscher, H. Antrekowitsch, H. Leitner, T. Ebner, P.J. Uggowitzer, Acta Mater. **59**, 3352 (2011)
[2] J. Hirsch, T. Al-Samman, Acta Mater. **61**, 818 (2013)
[3] J. Hirsch, Trans. Nonferrous Met. Soc. China **24**, 1995 (2014)
[4] G.A. Edwards, K. Stiller, G.L. Dunlop, M.J. Couper, Acta Mater. **46**, 3893 (1998)
[5] J.H. Chen, E. Costan, M.A. van Huis, Q. Xu, H.W. Zandbergen, Science **312**, 416 (2006)
[6] Y.X. Lai, B.C. Jiang, C.H. Liu, Z.K. Chen, C.L. Wu, J.H. Chen, J. Alloys Compd. **701**, 94 (2017)
[7] S.J. Andersen, H.W. Zandbergen, J. Jansen, C. TrÆholt, U. Tundal, O. Reiso, Acta Mater. **46**, 3283 (1998)
[8] W.C. Yang, M.P. Wang, R.R. Zhang, Q. Zhang, X.F. Sheng, Scripta Mater. **62**, 705 (2010)
[9] H. Zandbergen, S. Andersen, J. Jansen, Science **277**, 1221 (1997)
[10] F. De Geuser, W. Lefebvre, D. Blavette, Philos. Mag. Lett. **86**, 227 (2006)
[11] A. Serizawa, S. Hirosawa, T. Sato, Metall. Mater. Trans. A **39**, 243 (2008)
[12] H.S. Hasting, A.G. Frøseth, S.J. Andersen, R. Vissers, J.C. Walmsley, C.D. Marioara, F. Danoix, W. Lefebvre, R. Holmestad, J. Appl. Phys. **106**, 123527 (2009)
[13] S. Wenner, L. Jones, C.D. Marioara, R. Holmestad, Micron **96**, 103 (2017)
[14] L.P. Ding, Z.H. Jia, J.F. Nie, Y.Y. Weng, L.F. Cao, H.W. Chen, X.Z. Wu, Q. Liu, Acta Mater. **145**, 437 (2018)
[15] T. Saito, F.J.H. Ehlers, W. Lefebvre, D. Hernandez-Maldonado, R. Bjørge, C.D. Marioara, S.J. Andersen, R. Holmestad, Acta Mater. **78**, 245 (2014)
[16] T. Saito, S. Wenner, E. Osmundsen, C.D. Marioara, S.J. Andersen, J. Røyset, W. Lefebvre, R. Holmestad, Philos. Mag. **94**, 2410 (2014)
[17] N.N. Jiao, Y.X. Lai, S.L. Chen, P. Gao, J.H. Chen, J. Mater. Sci. Technol. **70**, 105 (2021)
[18] E.A. Mørtsell, C.D. Marioara, S.J. Andersen, J. Røyset, O. Reiso, R. Holmestad, Metall. Mater. Trans. A **46**, 4369 (2015)
[19] E.A. Mørtsell, S.J. Andersen, J. Friis, C.D. Marioara, R. Holmestad, Philos. Mag. **97**, 851 (2017)
[20] T. Saito, F.J.H. Ehlers, W. Lefebvre, D. Hernandez-Maldonado, R. Bjørge, C.D. Marioara, S.J. Andersen, E.A. Mørtsell, R. Holmestad, Scripta Mater. **110**, 6 (2016)
[21] T. Saito, C.D. Marioara, J. Røyset, R. Holmestad, Mater. Sci. Forum. **794**, 1014 (2014)
[22] Y.Y. Weng, Z.H. Jia, L.P. Ding, Y.F. Pan, Y.Y. Liu, Q. Liu, J. Alloys Compd. **695**, 2444 (2017)
[23] Y.Y. Weng, L.P. Ding, Z.Z. Zhang, Z.H. Jia, B.Y. Wen, Y.Y. Liu, S. Muraishi, Y.Y. Li, Q. Liu, Acta Mater. **180**, 301 (2019)
[24] Y. Liu, Y.X. Lai, Z.Q. Chen, S.L. Chen, P. Gao, J.H. Chen, J. Alloys Compd. **885**, 160942 (2021)
[25] M.A. Van Huis, J.H. Chen, H.W. Zandbergen, M.H.F. Sluiter, Acta Mater. **54**, 2945 (2006)
[26] M.A. Van Huis, M.H.F. Sluiter, J.H. Chen, H.W. Zandbergen, Phys. Rev. B **76**, 174113 (2007)
[27] Z.R. Liu, J.H. Chen, S.B. Wang, D.W. Yuan, M.J. Yin, C.L. Wu, Acta Mater. **59**, 7396 (2011)
[28] B. Zhang, L.L. Wu, B. Wan, J.W. Zhang, Z.H. Li, H.Y. Gou, J. Mater. Sci. **50**, 6498 (2015)
[29] Y. Zhang, D.W. Yuan, J.H. Chen, G. Zeng, T.W. Fan, Z.R. Liu, C.L. Wu, L.H. Liu, J. Electron. Mate. **45**, 4018 (2016)
[30] F.J.H. Ehlers, S. Dumoulin, J. Alloys Compd. **591**, 329 (2014)
[31] J. Peng, S. Bahl, A. Shyam, J.A. Haynes, D. Shin, Acta Mater. **196**, 747 (2020)
[32] G. Kresse, D. Joubert, Phys. Rev. B **59**, 1758 (1999)
[33] G. Kresse, J. Hafner, Phys. Rev. B Condens. Matter. Mater. Phys. **47**, 558 (1993)
[34] J.P. Perdew, Y. Wang, Phys. Rev. B **45**, 13244 (1992)
[35] H.J. Monkhorst, J.D. Pack, Phys. Rev. B **13**, 5188 (1976)
[36] F.H. Cao, J.X. Zheng, Y. Jiang, B. Chen, Y.R. Wang, T. Hu, Acta Mater. **164**, 207 (2019)
[37] L.H. Liu, Q.Q. Shao, T.W. Fan, D.W. Yuan, J.H. Chen, Comput. Mater. Sci. **198**, 110707 (2021)
[38] D.J. Siegel, L.G. Hector, J.B. Adams, Phys. Rev. B **65**, 085415 (2002)
[39] L.M. Liu, S.Q. Wang, H.Q. Ye, Acta Mater. **52**, 3681 (2004)
[40] W. Voigt, *Lehrbuch der Kristallphysik* (Taubner, Leipzig, 1928)
[41] A. Reuss, Z. Angew, Math. Mech. **9**, 49 (1929)
[42] R. Hill, Proc. Phys. Soc. London. Sect. A **65**, 349 (1952)
[43] M. Lei, H. Ledbetter, Y.F. Xie, J. Appl. Phys. **76**, 2738 (1994)
[44] S.F. Pugh, Philos. Mag. **45**, 823 (1954)
[45] D.W. Zhou, J.S. Liu, S.H. Xu, P.P. Peng, Comput. Mater. Sci. **86**, 24 (2014)
[46] E.A. Brandes, *Smithells metals reference book*, 6th edn. (Butterworts, London, 2002)
[47] F.J.H. Ehlers, R. Holmestad, Comp. Mater. Sci. **72**, 146 (2013)
[48] M. Born, K. Huang, M. Lax, Am. J. Phys. **23**, 474 (1955)
[49] Z.J. Wu, E.J. Zhao, H.P. Xiang, X.F. Hao, X.J. Liu, J. Meng, Phys. Rev. B **76**, 054115 (2007)